

Optically pumped GaN vertical cavity surface emitting laser with high index-contrast nanoporous distributed Bragg reflector

Seung-Min Lee,¹ Su-Hyun Gong,² Jin-Ho Kang,¹ Mohamed Ebaid,¹ Sang-Wan Ryu,^{1,3}
and Yong-Hoon Cho^{2,4}

¹Department of Physics, Chonnam National University, Gwangju 500-715, South Korea

²Department of Physics and KI for the Nano Century, Korea Advanced Institute of Science and Technology, Daejeon 305-701, South Korea

³sangwan@chonnam.ac.kr

⁴yhc@kaist.ac.kr

Abstract: Laser operation of a GaN vertical cavity surface emitting laser (VCSEL) is demonstrated under optical pumping with a nanoporous distributed Bragg reflector (DBR). High reflectivity, approaching 100%, is obtained due to the high index-contrast of the nanoporous DBR. The VCSEL system exhibits low threshold power density due to the formation of high Q-factor cavity, which shows the potential of nanoporous medium for optical devices.

©2015 Optical Society of America

OCIS codes: (140.7260) Vertical cavity surface emitting lasers; (160.4236) Nanomaterials; (230.1480) Bragg reflectors.

References and links

1. S. Nakamura, T. Mukai, and M. Senoh, "Candela-class high-brightness InGaN/AlGaIn double-heterostructure blue-light-emitting diodes," *Appl. Phys. Lett.* **64**(13), 1687–1689 (1994).
2. S. Nakamura, M. Senoh, S. Nagahama, N. Iwasa, T. Yamada, T. Matsushita, H. Kiyoku, Y. Sugimoto, T. Kozaki, H. Umemoto, M. Sano, and K. Chocho, "InGaN/GaN/AlGaIn-based laser diodes with modulation-doped strained-layer superlattices grown on an epitaxially laterally overgrown GaN substrate," *Appl. Phys. Lett.* **72**(2), 211–213 (1998).
3. A. Osinsky, S. Gangopadhyay, R. Gaska, B. Williams, M. A. Khan, D. Kuksenkov, and H. Temkin, "Low noise p- π -n GaN ultraviolet photodetectors," *Appl. Phys. Lett.* **71**(16), 2334–2336 (1997).
4. J. J. Hsieh, J. A. Rossi, and J. P. Donnelly, "Room-temperature cw operation of GaInAsP/InP double-heterostructure diode lasers emitting at 1.1 μ m," *Appl. Phys. Lett.* **28**(12), 709–711 (1976).
5. A. Gatto, A. Boletti, P. Boffi, N. Christian, M. Ortsiefer, E. Ronneberg, and M. Martinelli, "1.3- μ m VCSEL Transmission Performance up to 12.5 Gb/s for Metro Access Networks," *IEEE Photon. Technol. Lett.* **21**(12), 778–780 (2009).
6. S. T. Sanders, J. Wang, J. B. Jeffries, and R. K. Hanson, "Diode-laser absorption sensor for line-of-sight gas temperature distributions," *Appl. Opt.* **40**(24), 4404–4415 (2001).
7. A. V. Krishnamoorthy, K. W. Goossen, L. M. F. Chirovsky, R. G. Rozier, P. Chandramani, W. S. Hobson, S. P. Hui, J. Lopata, J. A. Walker, and L. A. D'Asaro, "16 x 16 VCSEL array flip-chip bonded to CMOS VLSI circuit," *IEEE Photon. Technol. Lett.* **8**, 1073–1075 (2001).
8. B. Weigl, M. Grabherr, C. Jung, R. Jager, G. Reiner, R. Michalzik, D. Sowada, and K. J. Ebeling, "High-performance oxide-confined GaAs VCSEL's," *IEEE J. Sel. Top. Quantum Electron.* **3**(2), 409–415 (1997).
9. T. Ive, O. Brandt, H. Kostial, T. Hesjedal, M. Ramsteiner, and K. H. Ploog, "Crack-free and conductive Si-doped AlN/GaN distributed Bragg reflectors grown on 6H-SiC(0001)," *Appl. Phys. Lett.* **85**(11), 1970–1972 (2004).
10. X. H. Zhang, S. J. Chua, W. Liu, L. S. Wang, A. M. Yong, and S. Y. Chow, "Crack-free fully epitaxial nitride microcavity with AlGaIn/GaN distributed Bragg reflectors and InGaIn/GaN quantum wells," *Appl. Phys. Lett.* **88**(19), 191111 (2006).
11. C. Berger, A. Dadgar, J. Blasing, A. Lesnik, P. Veit, G. Schmidt, T. Hempel, J. Christen, A. Krost, and A. Strittmatter, "Growth of AlInN/GaN distributed Bragg reflectors with improved interface quality," *J. Cryst. Growth*. in press., doi:10.1016/j.jcrysgro.2014.09.008.
12. T. Onishi, O. Imafuji, K. Nagamatsu, M. Kawaguchi, K. Yamanaka, and S. Takigawa, "Continuous Wave Operation of GaN Vertical Cavity Surface Emitting Lasers at Room Temperature," *IEEE J. Sel. Top. Quantum Electron.* **48**(9), 1107–1112 (2012).
13. M. C. Dixon, T. A. Daniel, M. Hieda, D. M. Smilgies, M. H. W. Chan, and D. L. Allara, "Preparation, Structure, and Optical Properties of Nanoporous Gold Thin Films," *Langmuir* **23**(5), 2414–2422 (2007).
14. E. V. Astrova and V. A. Tolmachev, "Effective refractive index and composition of oxidized porous silicon films," *Mater. Sci. Eng. B* **69–70**, 142–148 (2000).

15. L. A. Golovan, P. K. Kashkarov, and V. Y. Timoshenko, "Form birefringence in porous semiconductors and dielectrics," *Crystallogr. Rep.* **52**(4), 672–685 (2007).
16. J.-H. Lee, B. Lee, J.-H. Kang, J. K. Lee, and S.-W. Ryu, "Optical characterization of nanoporous GaN by spectroscopic ellipsometry," *Thin Solid Films* **525**, 84–87 (2012).
17. J. Park, J.-H. Kang, and S.-W. Ryu, "High Diffuse Reflectivity of Nanoporous GaN Distributed Bragg Reflector Formed by Electrochemical Etching," *Appl. Phys. Express* **6**(7), 072201 (2013).
18. R. J. Horowitz, H. Heitmann, Y. Kadota, and Y. Yamamoto, "GaAs microcavity quantum-well laser with enhanced coupling of spontaneous emission to the lasing mode," *Appl. Phys. Lett.* **61**(4), 393–395 (1992).
19. T. C. Lu, C. C. Kao, H. C. Kuo, G. S. Huang, and S. C. Wang, "CW lasing of current injection blue GaN-based vertical cavity surface emitting laser," *Appl. Phys. Lett.* **92**(14), 141102 (2008).
20. C. C. Kao, Y. C. Peng, H. H. Yao, J. Y. Tsai, Y. H. Chang, J. T. Chu, H. W. Huang, T. T. Kao, T. C. Lu, H. C. Kuo, S. C. Wang, and C. F. Lin, "Fabrication and performance of blue GaN-based vertical-cavity surface emitting laser employing AlN / GaN and Ta₂O₅ / SiO₂ distributed Bragg reflector," *Appl. Phys. Lett.* **87**(8), 081105 (2005).
21. J. Álvarez, P. Bettotti, I. Suárez, N. Kumar, D. Hill, V. Chirvony, L. Pavesi, and J. Martínez-Pastor, "Birefringent porous silicon membranes for optical sensing," *Opt. Express* **19**(27), 26106–26116 (2011).
22. S.-H. Gong, A. Stolz, G.-H. Myeong, E. Dogheche, A. Gokarna, S.-W. Ryu, D. Decoster, and Y.-H. Cho, "Effect of varying pore size of AAO films on refractive index and birefringence measured by prism coupling technique," *Opt. Lett.* **36**(21), 4272–4274 (2011).
23. B. Alshehri, S.-M. Lee, J.-H. Kang, S.-H. Gong, S.-W. Ryu, Y.-H. Cho, and E. Dogheche, "Optical waveguiding properties into porous gallium nitride structures investigated by prism coupling technique," *Appl. Phys. Lett.* **94**, 221907 (2014).
24. T. Yoshikawa, H. Kosaka, K. Kurihara, M. Kajita, Y. Sugimoto, and K. Kasahara, "Complete polarization control of 8×8 vertical-cavity surface-emitting laser matrix arrays," *Appl. Phys. Lett.* **66**(8), 908–910 (1995).

1. Introduction

Semiconductor optical devices have been developed with advances in compound semiconductor technology since 1960s, e.g., III-V and II-VI compounds, along with various types of optical devices, such as light-emitting diode [1], laser diode [2], and photodiode [3]. The performance of a semiconductor optical device relies on the available material combinations for controlling charge carrier transport as well as light propagation. For example, carrier confinement is achieved by constructing well-designed conduction/valence band profiles, whereas optical confinement is achieved by refractive index variation in a heterostructure [4]. An optical device with novel functionality and high efficiency can be manufactured only when its design fulfills the optical and electrical requirements by proper combination of available materials, which is the motivation for development of new materials and related heterojunctions. However, despite the strong efforts to grow new materials and improve their qualities, progress of optical device technology has been hindered by the lack of appropriate material in several areas, one of which will be discussed in the following.

A vertical cavity surface emitting laser (VCSEL) is a promising light emitter for short-reach data networks [5] and sensing applications [6]. VCSEL has advantages over conventional edge-emitting laser such as low threshold current, symmetric beam profile, on-wafer device testing, and the ability to be manufactured as a two-dimensional laser array [7]. A distributed Bragg reflector (DBR) is a key component of a VCSEL and the performance of DBR relies greatly on the available optical properties from materials compliant with the active media. For example, a VCSEL emitting at 850 nm exhibits low threshold current and superior efficiency, mainly due to the high quality factor (Q-factor) cavity formed by a GaAs/AlGaAs DBR [8]. The large index difference between GaAs and AlGaAs, the lattice constants of which are very closely matched, enables fabrication of high-performance DBRs, without the formation of crystalline defects. However, GaN VCSELs are limited by the lack of DBR pairs with reasonable optical and electrical properties [9]. A number of research groups have worked on the growth of various DBR pairs, including AlGaN/GaN [10] and InAlN/GaN [11]; however, these configurations suffer from low index-contrast, strain accumulation, and poor crystallinity. Dielectric DBRs offer an alternative approach, although their insulating nature complicates the design of electrically driven GaN VCSELs [12]. The poor performance of current GaN DBRs requires a new approach that can provide a large index-contrast, high electrical and thermal conductivities, and ease of manufacture.

Nano-porosification of bulk semiconductor material represents an interesting way to obtain the desired optical properties without development of new materials [13,14]. When the diameter of a nanopore is much smaller than the optical wavelength, the nanoporous material can be viewed as a homogeneous optical medium with modified refractive index; in this case, the Bruggeman effective medium approximation can be used to calculate the effective refractive index [15]. Based on this model, the controlled optical parameters resulting from varied porosities were demonstrated and analyzed previously [16]. The controllability of refractive index via nano-porosification will offer tremendous potential for designing optical devices under the limit of available materials. If there isn't a material with required optical parameters, we may manufacture it through nano-porosification from materials that we already have. Moreover, the nano-porosification can be selectively performed on layers to realize more complicated structures. In our previous work, a nanoporous etching technique of GaN was developed via electrochemical (EC) process which was doping-sensitive. A large index-contrast GaN DBR was fabricated from undoped-GaN/n-GaN multilayers by EC etching [17]. However, the DBR performance was not as good as theoretical simulation due to unoptimized etching conditions that caused the nonuniform formation of nanopores and limited stability of the structure. A second-order stopband was exhibited at ~450 nm, with maximum reflectivity of ~87%.

In this paper, we report the fabrication of a high-reflectivity (~100%) DBR by doping-selective nanoporous etching of undoped-GaN/n-GaN stacks. The improvement of maximum reflectivity was achieved based on more advanced EC etching for uniform and sturdy nanoporous GaN with newly developed electrolyte. This nanoporous DBR was adopted to realize a VCSEL cavity and continuous wave (CW) lasing action of the VCSEL through optical pumping was demonstrated at room temperature.

2. Experimental details

2.1 Fabrication of nanoporous DBR and VCSEL

The epitaxial layers of the VCSEL optical cavity were grown by metal-organic chemical vapor deposition. Growth started with deposition of a low-temperature GaN nucleation layer, followed by 1- μm -thick undoped GaN buffer. Nine pairs of n-GaN/undoped GaN (50 nm/50 nm) were grown, with n-type doping set at $5 \times 10^{18} \text{ cm}^{-3}$. Five pairs of InGaN quantum wells and GaN barriers were deposited, which were located at the center of a λ -cavity. Finally, eight pairs of n-GaN/undoped GaN were grown on the cavity to complete the epitaxial structure. The thickness of the topmost undoped GaN layer was increased to 130 nm to protect the wafer surface during subsequent EC etching. After deposition of 250-nm-thick SiO_2 layer, 350- μm -wide stripe patterns were formed with 50- μm -wide openings between them by conventional photolithography. The openings were mesa-etched by inductively coupled plasma reactive ion etching to expose the n-GaN sidewalls down to the undoped GaN buffer.

The processed samples were EC etched as anodes in 70% HNO_3 (wt/wt %) electrolyte for 5 minutes with a Pt wire as the counter electrode. EC etching started from the mesa sidewalls, and the etching voltage was varied between 15 and 19 V for the samples. The etch depth was monitored using optical microscopy by observing the changes in interference color. The etch depth increased linearly with time, but became saturated at ~50 μm due to insufficient electrolyte transport. Scanning electron microscopy (SEM) was used to examine the etching morphology; nanoporous GaN formation was observed for all samples. During EC etching, only n-GaN was etched due to its doping selectivity; thus, the undoped-GaN/n-GaN pairs were converted into bulk/nanoporous GaN pairs.

2.2 Optical characterization of nanoporous VCSEL

The reduced refractive index of a nanoporous layer formed high-reflectivity DBRs on the top and bottom of the λ -cavity, completing the VCSEL structure for optical pumping. The reflectivity spectra were measured by microspectrophotometer combined with an optical microscope. The light source was a tungsten-halogen lamp focused to a 10- μm light spot on

the sample surface with an objective lens ($40\times$). A half-mirror beamsplitter/combiner was inserted for illumination and to collect the reflected light from the sample. The experimental reflectivity spectra were fitted with thin-film simulation software (Essential Macleod ver. 9.8.437; Thin Film Center Inc.) to extract the structural parameters, such as the porosity and thickness of the DBR layers.

Optical pumping of the VCSEL samples was performed at room temperature using a semiconductor laser with a wavelength of 375 nm under CW operation. A microscope objective lens ($40\times$, numerical aperture: 0.5; Thorlabs) was used to excite an area of the VCSEL of approximately $1\ \mu\text{m}^2$ and to collect the emission from the samples in the normal direction. The emission spectrum was measured using a monochromator with a focal distance of 250 mm; equipped with a grating of 600 g/mm (SP2500i; Acton) and a charge-coupled device (CCD) detector. To eliminate the polarization dependence error from the optics system, we used a controlled half-wave plate in front of a fixed linear polarizer for polarization measurement.

3. Results and discussion

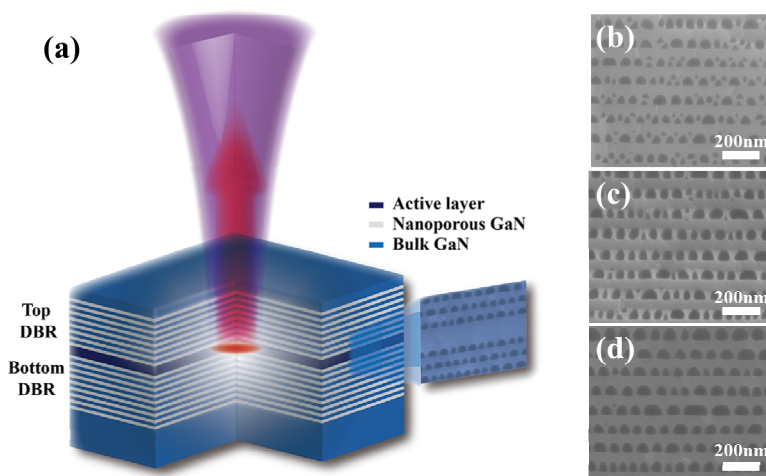


Fig. 1. (a) Schematic diagram of the GaN VCSEL structure with nanoporous DBRs. Cross-sectional SEM images of nanoporous DBRs etched in 70% HNO_3 at (b) 15 V, (c) 17 V, and (d) 19 V are displayed.

Figure 1(a) shows a schematic diagram of the fabricated VCSEL structure and its optical pumping geometry. The inset displays SEM image of the λ -cavity, sandwiched by nanoporous top and bottom DBRs. Figures 1(b)-1(d) show magnified SEM images of nanoporous DBRs formed at various EC etching voltages. Uniform nanopores were formed with HNO_3 electrolyte, and the DBR was free from damages such as warping and crack. The porosity increased with etching voltage (48%, 53%, 62% at 15, 17, and 19 V, respectively), which, in turn, decreased the refractive index of nanoporous GaN as 1.77, 1.69, and 1.56 from 2.47 for bulk GaN at 450 nm. Therefore, the porosity of the nanoporous GaN is an essential parameter that controls the stopband width and maximum reflectivity. A high EC etching voltage increased the porosity to enhance the high reflectivity of the DBR. However, an etching voltage above 20 V resulted in structural damage, such as warping and cracking in nanoporous GaN, due to the onset of complete etching.

The DBR pair was composed of two layers, i.e., bulk GaN (50 nm) and nanoporous GaN (50 nm). Because of the reduced refractive index of nanoporous layer, the optical thickness of each layer needed to be determined through the reflectivity simulation. The optical thickness of each layer was not exactly $\lambda/4$ in this work, however, the sum of optical thicknesses in a DBR pair was $\lambda/2$ at the designed wavelength.

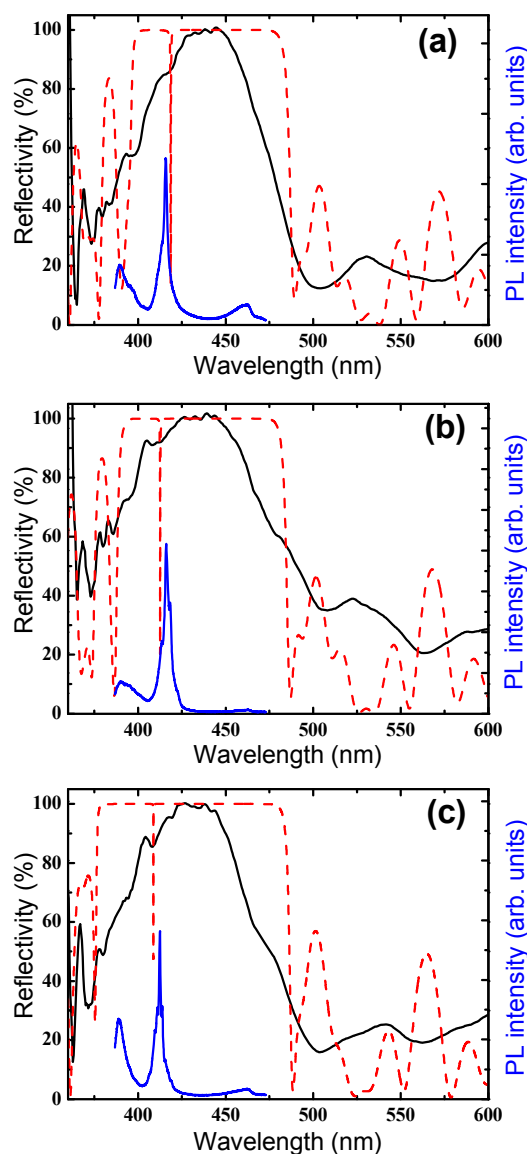


Fig. 2. Measured (solid line) and simulated (dashed line) reflectivity spectra of the GaN VCSEL with nanoporous DBRs, etched at (a) 15 V, (b) 17 V, and (c) 19 V. The blue lines represent μ -PL spectra from the corresponding VCSEL cavities.

Figure 2 shows the measured reflectivity curves (solid line) for samples etched at 15, 17, and 19 V, together with simulation results (dashed line). The experimental curve exhibited high reflectivity around 100% at the center of the stopband for all samples. The center wavelength of the stopband was ~ 440 nm, and the stopband width (reflectivity $> 90\%$) increased from 36 nm at 15 V to 38 nm at 19 V. A reflectivity dip was observed between 410 and 420 nm, which originated from resonant transmission through the high-reflectivity DBR, due to the cavity mode. The significant improvement in the DBR reflectivity compared to our previous report [17] was attributed to optimized EC etching conditions for nanoporification. An electrolyte in EC etching experiments is a critical parameter since it controls the formation of electrical double layer and reactions taking place at

semiconductor/electrolyte interface. The HNO₃ electrolyte enabled clear nanoporous etching, without damage to the undoped GaN; thus, high index-contrast DBR pairs could be fabricated without structural deformation. The nanopores were more uniform with the HNO₃ electrolyte, as shown in Fig. 1, which contributed to the high performance of the DBR.

Simulations on theoretical reflectivity spectra were conducted to fit the experimental curves, using the porosity values of nanoporous GaN measured in Fig. 1. During the simulation, the thickness of the DBR layers and λ -cavity were varied to obtain the simulated reflectivity spectra. The parameters were then adjusted until good agreement was achieved between the calculated and measured spectra in terms of the stopband center wavelength and resonance dip wavelength. The best fit was obtained with DBR pair thickness of ~ 102 nm and a λ -cavity thickness of ~ 160 nm, similar to the designed values. It should be noted that the measured reflectivity was significantly lower than the theoretical value at the edge of the stopband; this was attributed to the onset of diffuse scattering from the nonuniform distribution of nanopores in the nanoporous DBR. The randomized phase of scattered light deformed the stopband shape, especially at the edge.

Figure 2 displays microphotoluminescence (μ -PL) spectra measured from the samples together with reflectivity curves. The cavity mode from μ -PL was well matched with the dips in the reflectance spectra. The dips in the spectra were positioned within the high reflection stopband for the samples etched at 17 and 19 V, which was advantageous for formation of a high-Q cavity. However, the spectra of the sample etched at 15 V exhibited a deviation of the reflectivity dip from high reflectivity band due to its narrower stopband.

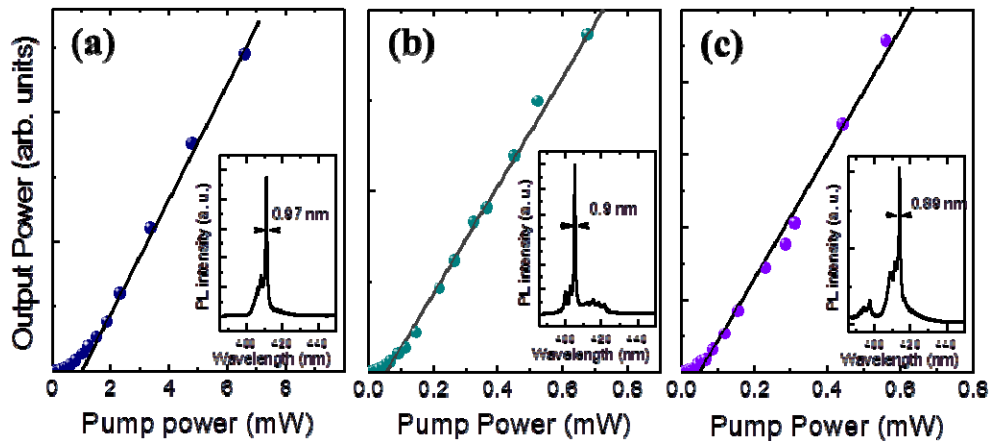


Fig. 3. Laser output intensity as a function of the pump power. The VCSELs were etched at (a) 15 V, (b) 17 V, and (c) 19 V. The insets show the laser emission spectra and associated linewidths.

Figure 3 shows room temperature lasing characteristics of the VCSEL samples in optical pumping experiments under CW operation; laser output intensity as a function of the pump power. Clear laser thresholds were observed for all samples. The emission intensity showed strong nonlinear behavior with respect to the pump power above the laser threshold. From linear fitting to the laser output curves, the laser threshold pump powers were 1067, 61, and 55 μ W corresponding to power densities of $\sim 1.36 \times 10^5$, 7.77×10^3 , and 7.05×10^3 W/cm², for VCSEL samples etched at 15, 17, and 19 V, respectively. The Q-factor of the cavity was evaluated by measuring the emission linewidth below the threshold, corresponding to 324, 425, and 446 for VCSEL samples etched at 15, 17, and 19 V, respectively. The emission linewidth was reduced above the pump threshold; the lasing spectra are shown in the inset of Fig. 3.

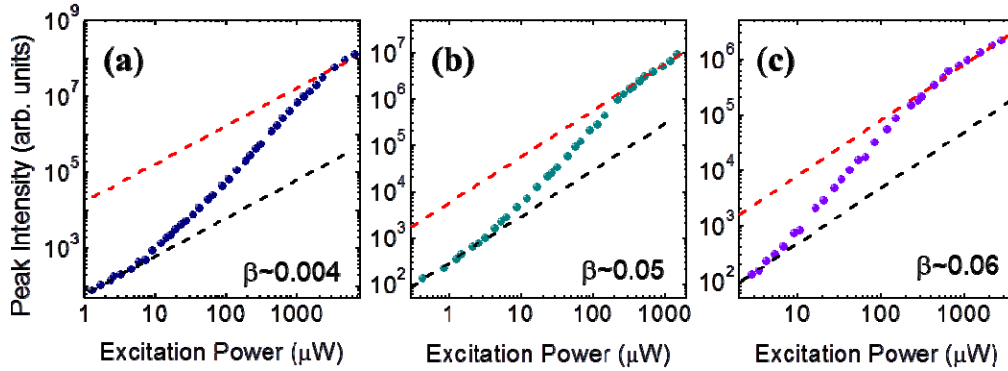


Fig. 4. Laser emission intensity as a function of the pump power, plotted on a logarithmic scale, fitted by the semiconductor rate equation for nanoporous VCSELs etched at (a) 15 V, (b) 17 V, and (c) 19 V.

The spontaneous emission coupling factor (β factor) was calculated from a log-log plot of the emission intensity as a function of the pump power, as shown in Fig. 4. The β value can be roughly estimated by the difference between the heights of the emission intensities, before and after lasing in the log-log plot [18]. The fitted β values were 4×10^{-3} , 5×10^{-2} , and 6×10^{-2} for VCSEL samples etched at 15, 17, and 19 V, respectively. With increasing etching voltage, the porosity of the n-type GaN layer increased, resulting in a high index-contrast for the DBR pair. The poor lasing behaviors (e.g., Q factor, laser threshold, and β factor) of the VCSEL etched at 15 V were due to the low porosity of nanoporous GaN. This reduced the stopband width, which caused deviation of the cavity resonance out of the DBR stopband. For etching voltages of 17 and 19 V, comparable VCSEL characteristics were achieved with only 8-9 pairs of DBRs, compared with the reported GaN-based VCSEL consisting of 25-28 pairs of GaN/AlN DBRs [19,20].

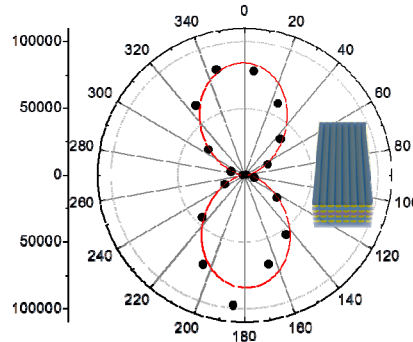


Fig. 5. Polarization characteristics of nanoporous VCSEL (black dot). The data were fitted by a sine function (red line). The inset was added to display the preferential polarization direction in connection with the nanopore propagation direction.

Figure 5 shows the polarization dependence of laser emission for the VCSEL etched at 19 V. A linear polarizer was installed in front of the VCSEL, and the polarization angle was varied for the measurement. The GaN-VCSEL, with a nanoporous DBR, displayed strong polarization dependence due to the anisotropic geometry of the nanopores. During EC etching, nanopores propagated in a direction normal with respect to the semiconductor/electrolyte interface, creating structural anisotropy in the DBR. The birefringent optical properties in structurally anisotropic materials were reported for porous Si [21], anodized alumina [22], and nanoporous GaN [23]. Due to the geometrical anisotropy of the DBR, the laser emission was linearly polarized along a direction parallel with respect to

the nanopores, resulting in a high polarization ratio of $R_p \sim 0.97$. R_p is defined as $R_p = (I_{\max} - I_{\min}) / (I_{\max} + I_{\min})$, where I_{\max} and I_{\min} are the maximum and minimum light intensity, respectively. Other VCSEL samples (those etched at 15 and 17 V) exhibited the same polarization dependence. This strong linear polarization behavior facilitates application of nanoporous DBR VCSELs in areas that require careful polarization control, such as magneto-optic recording and coherent detection systems [24].

The successful demonstration of optically pumped VCSEL operation with GaN-based materials paves a way to current injection VCSEL. The nanoporous DBR was examined to be current conducting though its electrical resistance was slightly increased. However, the doping dependence of EC etching allowed the formation of n-type DBR only. So, in a further study, a current injection VCSEL could be fabricated with n-type top and bottom DBRs and a tunnel junction between the active layer and one of the DBRs to draw hole current from the conduction band of n-GaN.

4. Conclusion

A nanoporous DBR GaN-VCSEL was fabricated by doping sensitive EC etching and its lasing characteristics were demonstrated by optical pumping. The nanoporous DBR exhibited high reflectivity (nearly 100%) for all EC etching conditions. As a result, the threshold lasing power density of nanoporous VCSEL was as low as $7-8 \times 10^3 \text{ W/cm}^2$, and the spontaneous emission coupling factor ranged from 0.05 to 0.06 for VCSELs etched at 17-19 V. These results, taken together with the high Q-factor, indicated that nanoporous GaN is advantageous to fabricate high-performance DBRs due to the controllability of refractive index.

Acknowledgments

S.-M. Lee and S.-H. Gong contributed equally to this work. This work was supported by the National Research Foundation of Korea (NRF) Grant funded by the Korean Government (NRF-2013R1A1A2059179).